12th International Conference on CANDU Fuel
Holiday Inn-Waterfront Hotel
Kingston, Ontario, Canada, 2013 September 15-18

Numerical Verification/Validation of the Theory of Coupled Reactors for Deuterium Critical Assembly, Using MCNP5 and Serpent Codes

M.S. Hussein[1], B.J. Lewis[2] & H.W. Bonin[3]

12th INTERNATIONAL CONFERENCE ON CANDU FUEL
Kingston, Ontario, Canada

[1,3]Department of Chemistry and Chemical Engineering
Royal Military College of Canada
(*P.O. Box 17000, Station Forces /Kingston, Ontario/K7K 7B4)*

[2]Faculty of Energy Systems and Nuclear Science University of Ontario Institute of Technology
(2000 Simcoe Street North, Oshawa, Ontario, Canada, L1H 7K4)

[1](613)5416000 ext.6181, mohamed.hussein@rmc.ca
[2](905) 721-3142 Brent.Lewis@uoit.ca
[3](613)541-6000 ext. 6613 bonin-h@rmc.ca

Abstract

The theory of multipoint coupled reactors developed by multi-group transport is verified by using the probabilistic transport code MCNP5 and the continuous-energy Monte Carlo reactor physics burnup calculation Serpent code. The verification was performed by calculating the multiplication factors (or criticality factors) and coupling coefficients for a two-region test reactor known as the Deuterium Critical Assembly, DCA. The multiplication factors k_{eff} calculated numerically and independently from simulations of the DCA by MCNP5 and Serpent codes are compared with the multiplication factors k_{eff} calculated based on the coupled reactor theory. Excellent agreement was obtained between the multiplication factors k_{eff} calculated with the Serpent code, with MCNP5, and from the coupled reactor theory. This analysis demonstrates that the Serpent code is valid for the multipoint coupled reactor calculations.

1. Introduction

Designing a multispectrum CANDU-based reactor as a possible actinides burner requires a numerical verification of the theory of coupled reactors using neutron transport codes. The validation of Serpent code for multipoint coupled reactors to employ it in the burnup calculations is required. The current verification and validation were performed by modeling the "Deuterium Critical Assembly (DCA)" using both the MCNP5 and Serpent codes to calculate multiplication factors and coupling coefficients for a two-region DCA test reactor. The term 'coupled' means that, in each of the regions, some of the fission neutrons are born in the other region. According to the verification of the MCNP5 and Serpent codes for designing multipoint coupled reactors, these two codes are indeed appropriate tools for advanced CANDU reactor design. The verification of the coupled reactors theory and these two codes confirms the possibility of using actinides as a fuel for the fast internal core of the multispectrum CANDU reactor designed for burning actinides.

The current Deuterium Critical Assembly model [1] consists of a two-region reactor. The inner core is a fast region fuelled by 2.7wt% U-235/U enriched uranium rods surrounded by light water. The outer core is the thermal region fuelled by 1.2wt% U-235/U enriched uranium rods

and moderated by heavy water. The internal region typically has a dominant fast neutron spectrum, while the external region has a dominant thermal one. Both regions would be independently subcritical on their own when the levels of light water and heavy water are at the mid height in both cores. The combination of the two regions is designed in such a way that the neutron leakage between them can provide sufficient reactivity to drive the combined system to criticality. The advantage of using the theory of coupled reactors consists in the fact that one can gain a better understanding in the multiplication factor for each region rather just for the whole system, which helps in improving the physical understanding of the detailed characteristics of the multispectrum system used as an actinide burner. The numerical verification of the coupled reactors theory for a Deuterium Critical Assembly using MCNP5 was performed by the authors in [2] where the results were compared with the TWOTRAN code [3] performed in the work of Nishihara [1].

The results from both models developed with MCNP5 and Serpent codes were validated and verified against a mathematical model based on coupled reactor theory.

The average percentage differences were calculated from Equation (1):

$$\Delta\%_{\substack{(MCNP5-Serpent)\ or;\\ Coupled\ Equation\ MCNP5\ or;\\ Coupled\ Equation\ Serpent}} = 100 \times \left(\frac{(k_{eff})_{\substack{MCNP5\ or;\\ MCNP5\ or;\\ Serpent}} - (k_{eff})_{\substack{Serpent\ or;\\ Coupled\ Equation\ MCNP5\ or;\\ Coupled\ Equation\ Serpent}}}{(k_{eff})_{\substack{MCNP5\ or;\\ MCNP5\ or;\\ Serpent}}} \right) \quad (1)$$

An excellent agreement of the Serpent numerical model over the MCNP5 results of k_{eff} with an average percentage ratio of 0.6% is displayed. The outstanding agreement between both the MCNP5 and Serpent results of k_{eff} over the corresponding calculations of the coupled equations is 0.4% and 0.6%, respectively.The validation of Serpent code for coupled reactor calculations provides the advantages that it can be used in the burnup calculations for a multispectrum CANDU-based reactor. MCNP5 and Serpent codes therefore represent valid tools for modelling coupled reactors.

2. The Research Approach

The theory of a coupled reactor was first pioneered by Avery [4], [5], and [6]. The theory was modified and extended by Komata [7], Kobayashi [8] and Nishihara [1]. A brief mathematical formulation of the nodal equations of the coupled reactor system was derived by Kobayashi [8]. For this two-region reactor model, one can obtain easily the multiplication factor k_{eff} which is related to regional criticality factors k_{11} and k_{22}, and the coupling coefficients k_{12} and k_{21} by Equation (2):

$$k_{eff} = \frac{1}{2}\left[k_{11} + k_{22} + \sqrt{(k_{11} - k_{22})^2 + 4k_{12} \cdot k_{21}}\right] \quad (2)$$

The coupling coefficients are defined by Allen [9] as

$$k_{12} = \frac{R_{f,1\leftarrow 2}}{(R_{f,1} + R_{f,2})} \times k_{eff} \quad (3)$$

$$k_{21} = \frac{R_{f,2\leftarrow1}}{(R_{f,1} + R_{f,2})} \times k_{eff} \quad (4)$$

where
$R_{f,1}$:is the fission rate in the inner region or the fast core (fission cm^{-3} s^{-1}),
$R_{f,2}$:is the fission rate in the outer region or the fast core (fission cm^{-3} s^{-1}),
$R_{f,1\leftarrow2}$: is the fission rate in the inner region triggered by neutrons born in the outer region (fission cm^{-3} s^{-1}),
$R_{f,2\leftarrow1}$: is the fission rate in the outer core triggered by neutrons born in the inner region (fission cm^{-3} s^{-1});
k_{11}: is the average number of next generation fission neutrons in the inner fast region resulting from a single fission neutron born in the inner fast region,
k_{22}:is the average number of next generation fission neutrons in the outer thermal region resulting from a single fission neutron born in the outer thermal region,
k_{21}: is the average number of next generation fission neutrons in the outer thermal region resulting from a single fission neutron born in the inner fast region, and
k_{12}: is the average number of next generation fission neutrons in the inner fast region resulting from a single fission neutron born in the outer thermal region.

In Equations (3) and (4), the sum in the denominator represents the fission rate in the inner region $R_{f,1}$ plus the fission rate in the outer region $R_{f,2}$ that is equal to the total fission rate as directly related to the effective multiplication factor k_{eff} of the whole system. The ratio of either $R_{f,1\leftarrow2}$ and $R_{f,2\leftarrow1}$ over the total fission rate represents the fraction of the k_{eff} value which corresponding to the contribution of one region to the other. All fission rates values used in the k_{12} and k_{21} formula, Equations (3) and (4), are calculated from the neutron fluxes results from using the F4 flux tally and the CF4 flagging tally given in the MCNP5 using Equations (5) and (6). The flagging flux of the thermal core is defined as the part of the flux contributed from thermal core and having passed to the fast core. The flagging cell used is the air gap cell, cell 5.

In the present work, the probabilistic computer code MCNP5 (Monte Carlo N-Particle) [10] and Serpent (continuous-energy Monte Carlo reactor physics burnup calculation code) are used to simulate the DCA experiment for which two similar models were designed. The nuclear data library used with both MCNP5 and Serpent is ENDF/B-VII. The criticality factors k_{eff}, k_{11} and k_{22} were computed with both MCNP5 and Serpent along with the coupling coefficients k_{12} and k_{21} from Equations (3) and (4). The coupling between the two DCA regions is validated by comparing k_{eff} as calculated by Equation (2) with that computed directly by MCNP5 and Serpent.

3. Heavy Water Critical Assembly (DCA)

The DCA has a cylindrical geometry shape with an outer radius of 150.25 cm. It consists of two reactor core regions. The inner and outer regions are separated by an air gap of thickness 9.2 cm as shown in Figure 1. The inner region is loaded with 2.7wt% U-235/U enriched metallic uranium fuel rods in aluminum clad surrounded by light water coolant. The lattice pitch of the fast core is designed as small value (1.9 cm) to minimize the moderation of the fast neutrons by light water as much as possible. The outer region is loaded with 1.2 wt% U-235/U enriched uranium rods in aluminum clad of thickness 1.4 mm surrounded by heavy water. The thermal core lattice was optimized to a 474 fuel clusters in a square lattice cells with a thermal lattice pitch of 9.66 cm [2]. Each cluster has four fuel rods for total of 1896 fuel rods [2]. In the outer thermal core the heavy water is used as moderator and coolant. The inner region consists of 140

fuel rods distributed within a square lattice with a lattice pitch=1.9 cm. The middle cell of the inner region consists in an air tube of inner radius 1.5 cm and an aluminum wall of thickness 0.2 cm. The inner core consists in an aluminum cylinder of inner radius 16.8 cm and outer radius 17.5 cm. The inner radius of the outer core is 33.851 cm and the outer radius is 133.875 cm. The outer core is surrounded by two heavy water reflectors. The outer reflector thickness is 16.375 cm and the inner reflector thickness is 4.351 cm. In both cores, the fuel rod diameter is 1.45 cm and its length is 200 cm. The fuel rods are cladded in aluminum tubes of 1.4 mm thickness. More details and dimensions are shown in Figure 1 of the MCNP5 model and Figure 2 of the Serpent model. The inner region or the fast core is designated as Core 1 and the outer region or thermal core is referred to as Core 2.

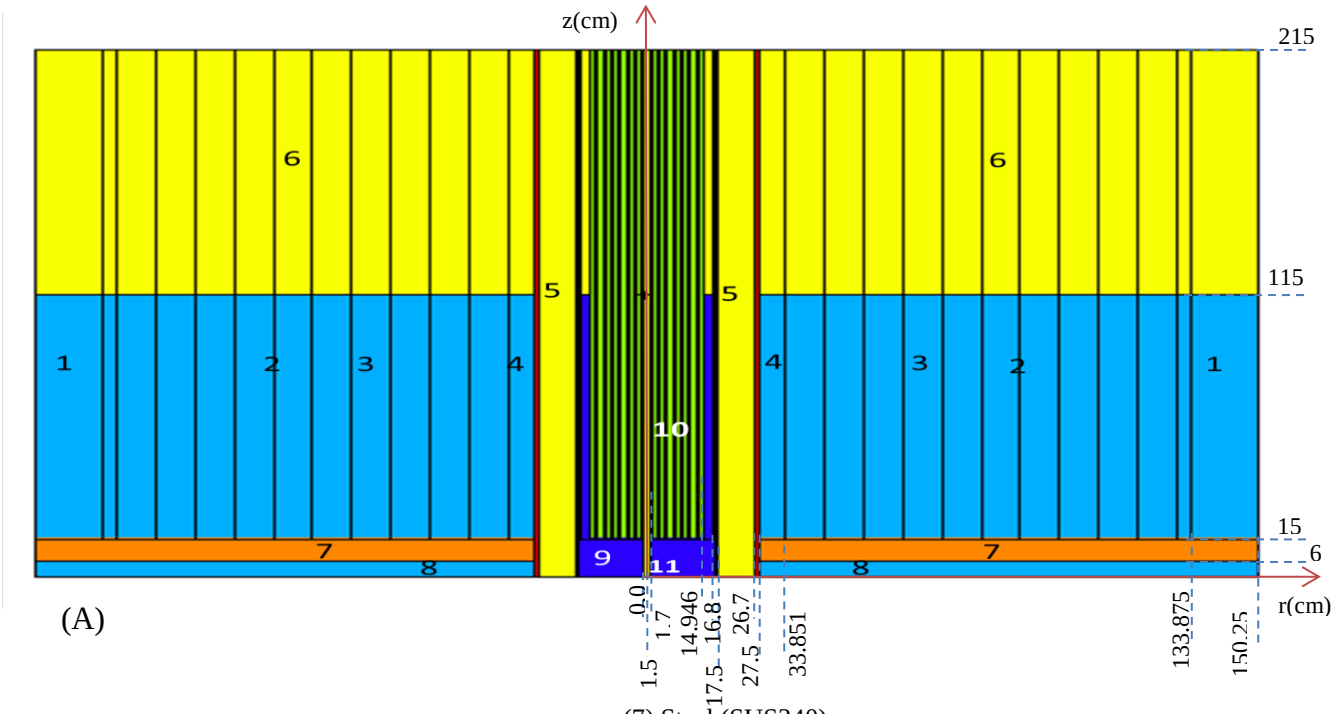

(1) Heavy water external reflector.
(2) Thermal core fuel lattice.
(3) Heavy water moderator and coolant
(4) Internal heavy water reflector.
(5) Air gap
(6) Air above the thermal core
(7) Steel (SUS340)
(8) Heavy water.
(9) Light water in the fast core (coolant)
(10) Fast core fuel lattice.
(11) Aluminum tube in the middle of the fast core of wall thickness 0.2 mm .It contains air.

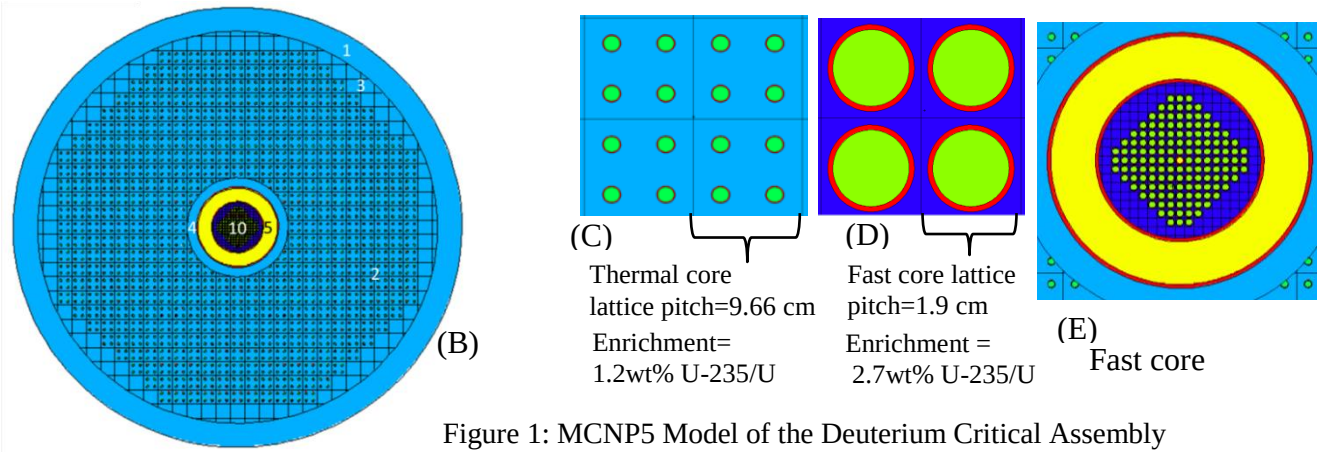

Figure 1: MCNP5 Model of the Deuterium Critical Assembly

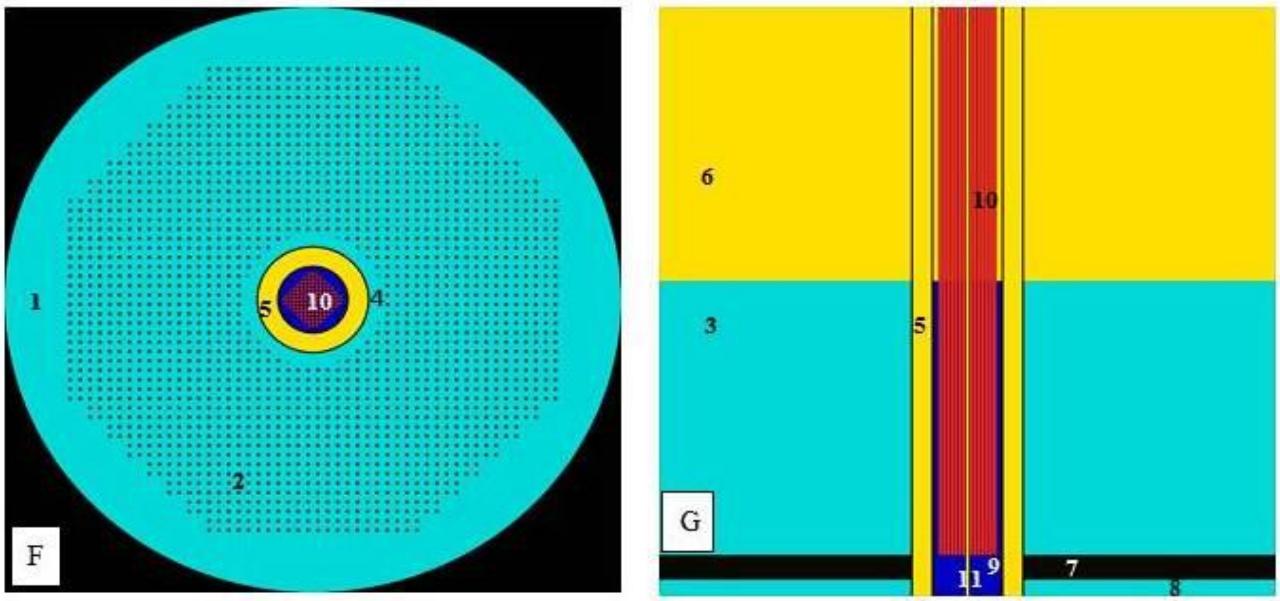

(1) Heavy water external reflector.
(2) Thermal core fuel lattice.
(3) Heavy water moderator and coolant
(4) Internal heavy water reflector.
(5) Air gap
(6) Air above the thermal core
(7) Steel (SUS340)
(8) Heavy water.
(9) Light water in the fast core (coolant)
(10) Fast core fuel lattice.
(11) Aluminum tube in the middle of the fast core of wall thickness 0.2 mm .It contains air.

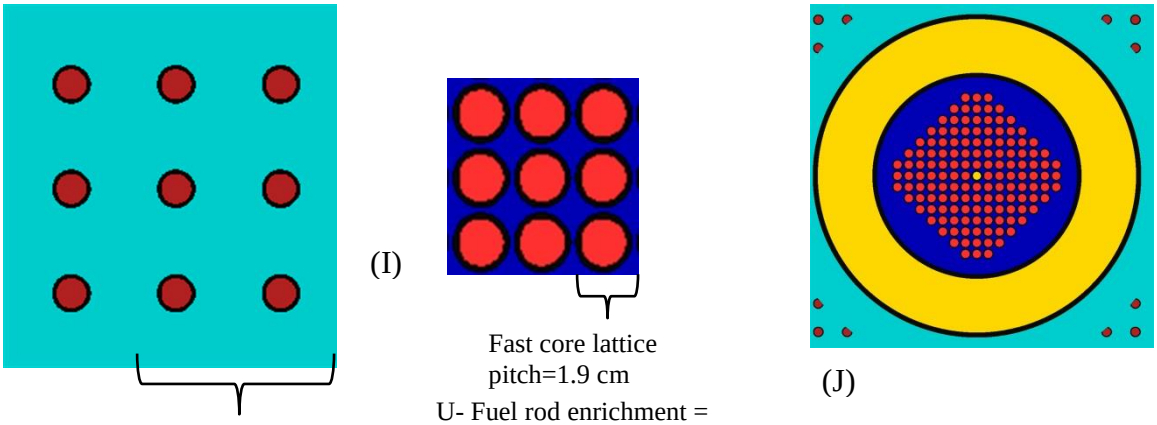

(H)

Thermal core lattice pitch=9.66 cm

U- Fuel rod enrichment=1.2wt% U-235/U

(I)

Fast core lattice pitch=1.9 cm

U- Fuel rod enrichment = 2.7wt% U-235/UU- Fuel

(J)

Fast core lattice

For both cores, Al-clad thickness =1.4 mm, diameter of rod = 1.45cm and length of the fuel rod= 200 cm

Figure 2: Serpent Model of the Deuterium Critical Assembly

3.1. Design and Simulation of the Two Regions DCA with Exact Dimensions and Optimal Components using MCNP5 and Serpent Codes

Components (A) and (B) of Figure 1 and (F) and (G) of Figure 2 show the vertical and horizontal cross sections of the DCA model for a level of heavy water and light water in the thermal and fast regions set at 100 cm on the MCNP5 and Serpent models. Figure 1 (C), (D) and (E), and Figure 2 (H), (I) and (J) show close-up views of the lattice pitch of the thermal and fast cores model simulated using MCNP5 and Serpent code respectively.

Due to the limitation of the Serpent code for temperatures less than 300K, the temperature in the Serpent code is set at 300K while the temperature of the MCNP5 code is set to the closest value in the chosen library at 293.6 K. Some of the MCNP5 models were run at 300K but there is no significant differences have been detected due this small temperature difference.

The models were optimized to realize DCA criticality condition which is each of fast core and thermal core should be subcritical independently when the levels of light water and heavy water are at 100 cm height. In both simulation models, to calculate k_{11} and $k_{22,}$ the air gap, (cell 5, Figure 2 and Figure 3), is included. The reason of the air gap involvement in the simulations of thermal core, through k_{22} calculations, is to consider the neutrons which may escape from the thermal core and back to it through the air gap. Consequently, to realize the DCA criticality condition, the aluminum clad thickness in the whole DCA was adjusted to the value of 1.4 mm in both models.

4. Methodology

As the DCA model was optimized, the coupling reactor theory was verified by driving the system to criticality. Different values of criticality factors k_{eff}, k_{11} and k_{22} and corresponding values of coupling coefficients k_{12} and k_{21} were calculated by changing the level of heavy water in the thermal region and setting the light water level at 100 cm in the fast region, and vice versa. The simulation steps can be summarized as follows:

1- To find the optimum value of the number of cycles and number of neutrons per cycle to be used in the criticality calculations, both DCA models designed by MCNP5 and Serpent codes were run at different number cycles with different number of neutrons per cycle as shown in Figure 3. These simulations are run for the cases of the both light water and heavy water at 100 cm in the fast and thermal core. The best convergence of k_{eff} value was obtained for the number of neutrons and the number of cycles set at 5000 n cycle and 500 cycles respectively. These values represent the first converging value of k_{eff}.

2- The criticality factors k_{11} were calculated by setting the importance of neutrons in the thermal core to zero value in the MCNP5 DCA models. The equivalent setting in the Serpent DCA model the thermal core is set as "outside universe". In both cases the neutron histories will be killed as the neutron crosses to the thermal core region. In this case, calculating the k_{eff} of the system represents only the criticality factors k_{11} of the fast region. Similarly, coupling coefficients k_{22} were calculated by setting the importance of the neutrons in the fast core to a value of zero in the MCNP5 DCA model or, as an "outside universe" in the DCA Serpent model. The air gap region, cell 5, was included in the two models during k_{22} calculation to account for the neutrons that escape from the thermal core and back to it after passing through the air gap.

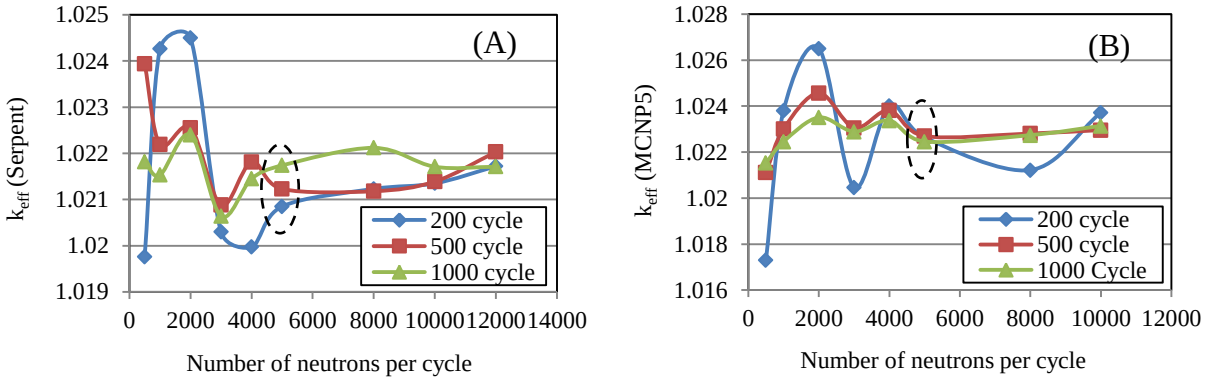

Figure 3: The Convergence Value of k_{eff} with the Number of Cycles and Number of Neutron Per Cycle Using Serpent (Figure 3-A) and MCNP5 (Figure3- B).

3- The criticality factor k_{11} is calculated for various levels of light water in the fast core. Similarly, the criticality factor k_{22} is calculated for various levels of heavy water in the thermal core.

4- The two regions of the DCA models were simulated by MCNP5 and by Serpent at different levels of heavy water in the thermal core and light water in the fast core. The multiplication factors k_{eff} for the corresponding k_{11} and k_{22} were calculated at each level of heavy water with setting the light water at 100 cm and vice versa.

5- From the two region simulations, the normalized flux in each region was calculated by using the F4 tally in the MCNP5 [10] and cell flux detector in Serpent code. This normalized flux represented in Figures 4,5,6, and 7 is the fluence or the flux times one second. The actual flux can be calculated using Equation (2) in Reference [11]. The actual flux is not relevant to the current work because the values of k_{12} and k_{21} depend on the fluxes ratio as shown in Equations (3) and (4). The normalized cell flux and the flagging flux were calculated for three energy groups; thermal, epithermal and fast, corresponding to energy ranges from 10^{-11} eV to 0.625 eV, 0.625 eV to 0.1 MeV and 0.1 MeV to 14 MeV, respectively.

6- The total reaction rates $R_{f,1}$ and $R_{f,2}$ in each core could be calculated through Equation (5) where $\varphi_1(E_i)$ and $\varphi_2(E_i)$ could be defied as follows: (A) The normalized flux $\varphi_1(E_i)$ is the flux in the fast core, which is due to the fission in the fast core plus the contribution of the neutrons flux $\varphi_1(E_i)_{1\leftarrow 2}$ as diffused from the thermal core to the fast one for an energy E_i and (B) the normalized flux $\varphi_2(E_i)$ is the flux in the thermal core, which is due to the fission in the thermal core plus the contribution of the flux $\varphi_2(E_i)_{2\leftarrow 1}$ diffused from the fast core to the thermal one.

7- For the DCA model simulated with MCNP5, the flagging cell tally CF4 [10] is the neutron flux for the three considered energy groups that diffuse from the thermal region to the fast region, and the reverse could be calculated. This flagging cell flux $\varphi_1(E_i)_{1\leftarrow 2}$ is the normalized flux that can diffuse from the thermal core and contributes to the criticality factor of the fast core k_{11} for the energy group "i". The flagging flux $\varphi_2(E_i)_{2\leftarrow 1}$is the normalized flux that can diffuse from the fast core and contributes to the criticality factor of the thermal core k_{22} for the energy group "i".

8- The average fission cross sections were calculated for each neutron energy group (thermal, epithermal and fast). The fission reaction rates $R_{f,1\leftarrow 2}$ and $R_{f,2\leftarrow 1}$were also calculated from Equations (5) and (6). The coupling coefficients k_{21} and k_{12} could be calculated from Equation (3) and (4) respectively. On the other hand, in the DCA model simulation by Serpent, the fluxes, $\varphi_1(E_i)$ and $\varphi_2(E_i)$ could be calculated using the cell detector of both fast and thermal core respectively. Consequently, $R_{f,1}$ and $R_{f,2}$ could be calculated.

$$R_{f,n} = \left(N_D(U_{235})\sum_i^3[\sigma_f(E_i)\times\varphi_n(E_i)]\right) + \left(N_D(U_{238})\sum_i^3[\sigma_f(E_i)\times\varphi_n(E_i)]\right) \quad (5)$$

$$R_{\substack{f,1\leftarrow 2\\ or\ 2\leftarrow 1}} = \left(N_D(U_{235})\sum_i^3\left[\sigma_f(E_i)\times\varphi_{\substack{1\leftarrow 2\\ or\ 2\leftarrow 1}}(E_i)\right]\right) + \left(N_D(U_{238})\sum_i^3\left[\sigma_f(E_i)\times\varphi_{\substack{1\leftarrow 2\\ or\ 2\leftarrow 1}}(E_i)\right]\right) \quad (6)$$

9- Due to the limitation of Serpent for the flagging cell flux detector definition and because of the strong agreement between the fluxes in fast core $\varphi_1(E_i)$ and thermal core $\varphi_2(E_i)$ calculated by MCNP5 and those calculated by Serpent, as shown in Figure 4,Figure 5, Figure 6 and Figure 7, the flagged waiting flux from MCNP5 could be used to calculate the flagging flux in Serpent. These flux values are normalized per number of neutrons history and volume. The flagging flux from the thermal core in the air gap cell 5 in Serpent, $\varphi_n(E_i)_{1\leftarrow 2}(Serpent)$, could be calculated by multiplying the thermal flux of core $\varphi_2(E_i)$ from Serpent times the ratio between the flagging flux $\varphi_n(E_i)_{1\leftarrow 2}(MCNP)$ and the thermal flux of core $\varphi_2(E_i)(MCNP)$. This ratio is called flagged waiting flux as shown in Equations (7). The same method is used to calculate the flagging flux from the fast core to the thermal one:

$$\varphi_n(E_i)_{\substack{1\leftarrow 2\\ or\ 2\leftarrow 1}}(Serpent) = \frac{\varphi_n(E_i)_{\substack{1\leftarrow 2\\ or\ 2\leftarrow 1}}(MCNP)}{\varphi_n(E_i)\ (MCNP)} \times \varphi_n(E_i)\ (Serpent) \quad (7)$$

10- The multiplication factors k_{eff} calculated from coupling Equation (2), based on the values of criticality factors k_{11}, k_{22}, and coupling coefficients k_{12}, k_{21} from both MCNP5 and Serpent codes, were compared with the multiplication factors k_{eff} that were calculated numerically and independently by both MCNP5 and Serpent codes for the system as a whole, for different levels of heavy and light water in the two regions.

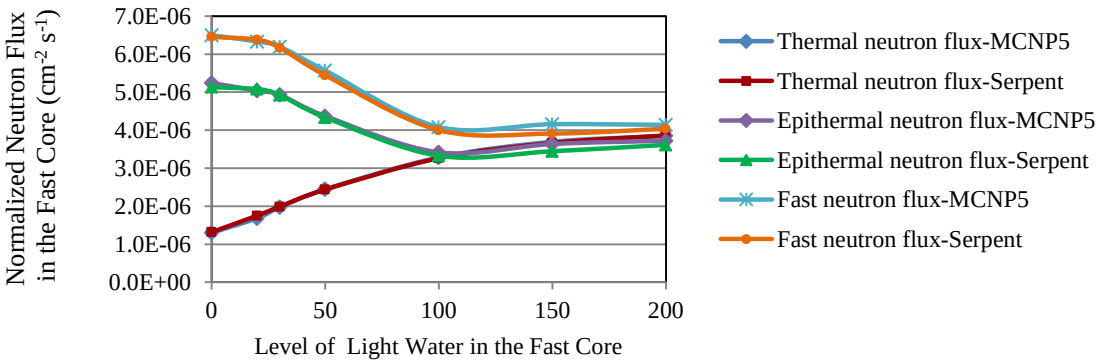

Figure 4: Variations of the Normalized Fluxes in the Fast Core at Different Levels of Light Water in the Fast Core, at 100 cm of the Heavy Water Level in the Thermal Core.

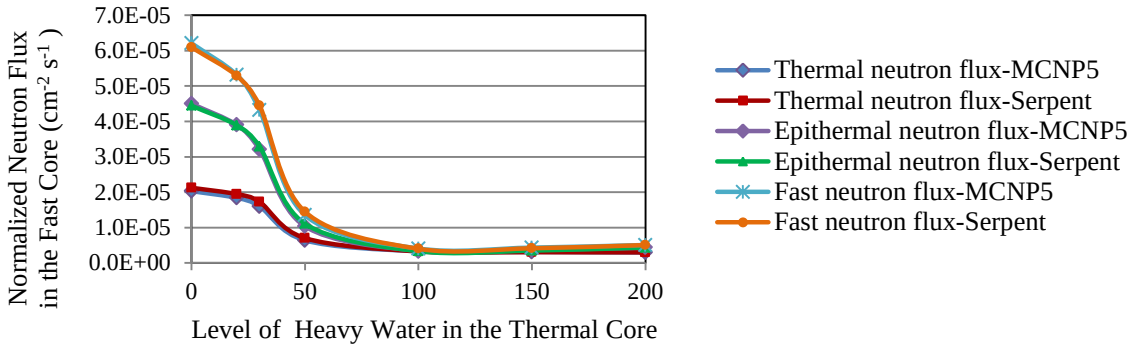

Figure 5: Variations of the Normalized Fluxes in the Fast Core at Different Levels of Heavy Water in the Thermal Core, at 100 cm of the Light Water Level in the Fast Core.

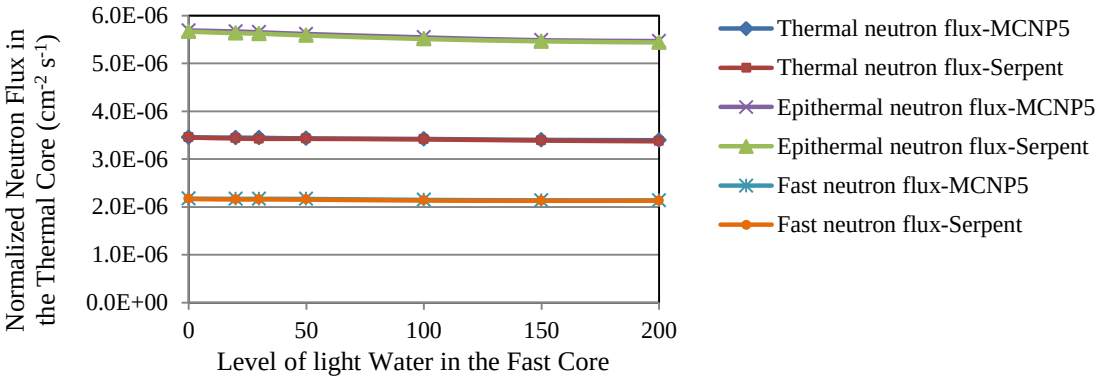

Figure 6: Variations of the Normalized Fluxes in the Thermal Core at Different Levels of Light Water in the Fast Core, at 100 cm of the Heavy Water Level in the Thermal Core.

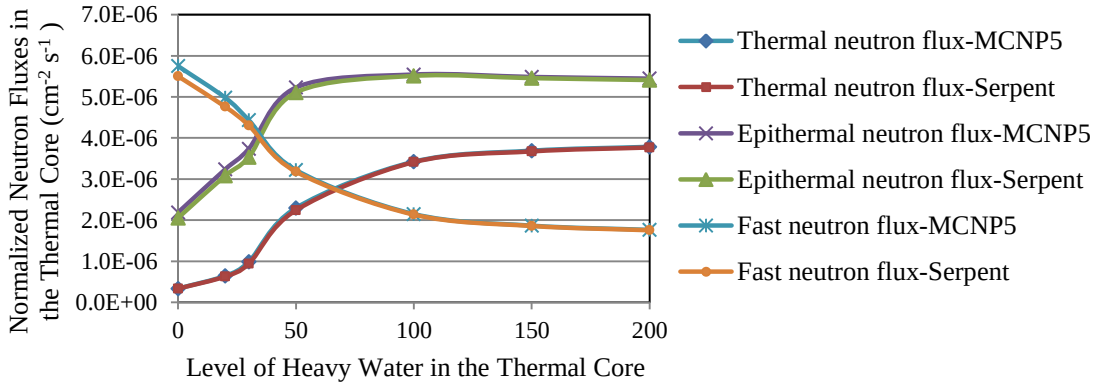

Figure 7: Variations of the Normalized Fluxes in the Thermal Core at Different Levels of Heavy Water in the Fast Core, at 100 cm Of The Light Water Level in the Fast Core.

where, i=1,2 or 3 represent the energy bin of thermal, epithermal or fast respectively and, n=1 for the fast core flux and n=2 for the thermal core flux.

11- The fluxes in Figure 4, Figure 5, Figure 6 and Figure 7 represents the fluxes given by the tally F4 in the MCNP5 and cell flux detector in Serpent. These fluxes are normalized per unit volume and number of history.

5. Results and Discussion

1- From Figure 4, Figure 5, Figure 6, and Figure 7, one can notice an excellent agreement between the behaviour of the fluxes calculated from the MCNP5 and the Serpent codes. Therefore the following discussion for these figures is applicable to the flux results from both codes.

2- Figure 4 represents the change of the three groups' fluxes in the thermal core with increasing the level of the light water in the fast core. One can notice that, as the light water level increases, the fast and epithermal groups fluxes are decreasing due to the moderation effect of the light water. Consequently, the thermal group fluxes increase gradually. Above 100 cm, the thermal group fluxes and the epithermal group fluxes are increasing very slowly while the fast group fluxes are almost constant. This small increase in the thermal and epithermal groups are due to more moderation as the level of the light water increases. The other effects on the thermal and epithermal groups are the mutual effects from the thermal core because, as the light water increases, more moderation occurs to the diffused neutron from the thermal core which increases the thermal flux in the fast core.

3- Figure 5 represents the effect due to changing of the heavy water in the thermal core on the three group fluxes in the fast core. As the heavy water level increases, the three groups' fluxes decrease. The fast and epithermal groups are decreasing strongly due to the effect of the strong moderation of heavy water. Consequently, more absorption, fission and radioactive capture occur in the thermal core. Therefore the thermal flux in the fast core also decreases. All energy groups fluxes will come to stability when the level of heavy water exceeds above 100 cm because the rate of fission is almost equal to the rate of absorption and moderation. Consequently the three groups' fluxes that diffuse from the thermal core to the fast core become essentially constant.

4- In Figure 6, as the light water level increases in the fast core, the only significant change in the fluxes in the thermal core occurs for the epithermal flux. This is due to the moderation effect of the light water. The other groups' fluxes are not significantly changed due to the big difference between the volumes and amount of the fuel the fast and thermal cores.

5- From Figure 7, one can notice, as the heavy water level increases in the thermal core, the fast neutron flux level decreases due to the moderation effect of heavy water. The epithermal and thermal fluxes increase and come to constant values for a 150 cm level of heavy water when the rates of moderation from fast to epithermal and from epithermal to thermal group were almost the same.

6- From Figure 8, one can notice the consistency of the criticality factors k_{11}, k_{22} and coupling coefficients k_{12} and k_{21} as calculated with MCNP5 and Serpent. Consequently, the multiplication factors k_{eff} as calculated with the coupled reactor Equation (2) by these values independently from each code strongly match.

7- Figure 9 represents the comparison between the multiplication factors k_{eff} calculated directly by both MCNP5 and Serpent and that calculated by the coupled reactor equation. One can notice that the behaviours of the k_{eff} curves calculated by the two codes are very similar. This is also true for the k_{eff} calculated from the coupled reactor theory. Table (1) presents the average percentage difference between the k_{eff} calculated by MCNP5 and Serpent and from the coupled reactor theory.

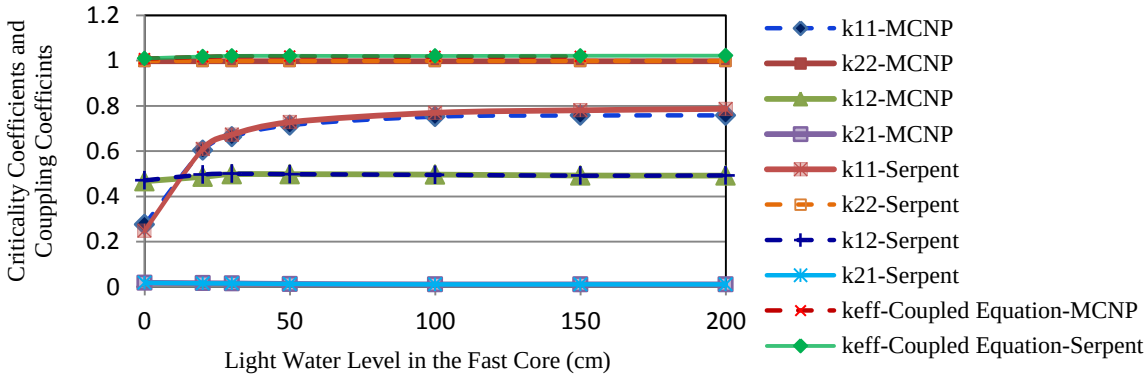

Figure 8: Criticality Factors and Coupling Coefficients at Different Light Water Levels in the Fast Core with the Heavy Water Level at 100 cm in the Thermal Core Calculated by Serpent, MCNP5 Codes and Coupled Reactor Equation.

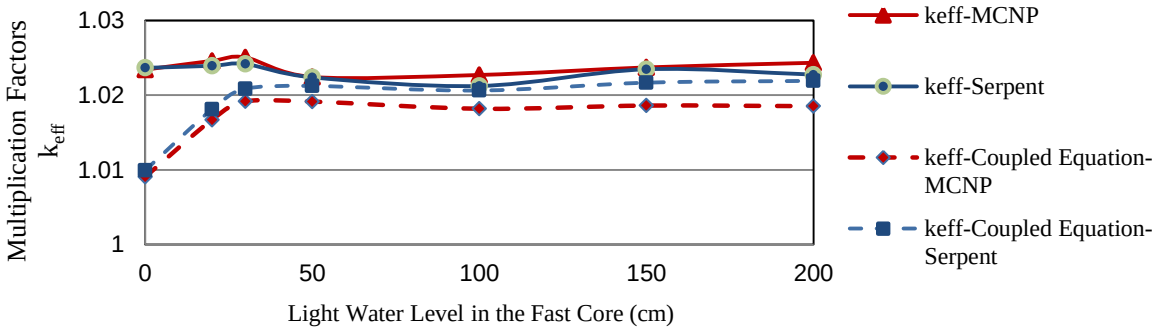

Figure 9: Multiplication Factors k_{eff} at Different Light Water Levels with Heavy Water at 100 cm Calculated by Serpent and MCNP5 and the Coupled Reactor Equation.

Table 1: Average Percentage Difference between k_{eff} as Calculated by MCNP5, Serpent and the Coupled Reactor Theory.

	$\%\Delta k_{eff}$ (MCNP5-Serpent)	$\%\Delta k_{eff}$ (MCNP5-Coupling theory)	$\%\Delta k_{eff}$ (Serpent-Coupling theory
Average percentage of difference k_{eff} when setting the levels of heavy water at 100 cm and change the level of the light water from 0 to 200 cm	0.07%	0.65%	0.38%
Average percentage of difference k_{eff} when setting the levels of light water at 100 cm and change the level of the heavy water from 0 to 200 cm	1.04%	0.54%	0.43%

8- Figure 10 (A) and (B) represent close-ups of the criticality factors k11 and k22. One can notice that, as the light water level increases in the fast core, the value of k22 is not affected because it was calculated when the thermal core was switched off. The criticality factors k22 from MCNP5 and Serpent in good agreement with a difference of 0.13%. On the other hand, the criticality factor k11 strongly increases as the light water level increases because of the moderation effect. As the light water level increases to 30 cm height, the rate of increasing k11 decreases gradually due to the absorption effect of the light water. The factor k11 become constant at light water level of 100 cm and above because the rates of fission become equal to the rates of absorption and leakage from the core. The criticality factors k11 from MCNP5 and Serpent are very much in good agreement with a difference of 3.28%.

9- Figure 11 (A) and (B) are close-ups of the coupling coefficients k12 and k21 as the light water level increases in the fast core. The coupling coefficient k12 increases sharply due to the effect of the moderation of the light water on the neutrons diffusing from thermal to the fast core, but as the light water level increases above 50 cm; the coupling coefficient the k12 starts to decrease gradually due to absorption effect of the light water.

10- The coupling coefficient k_{12} becomes constant at the 150 cm level and above because the rate of neutron absorption by the light water becomes equal to that of the neutrons diffused from the thermal core.

11- On the other hand, Figure 11 (B) represents the criticality factor k_{21} which decreases gradually until the level of the light water reaches at 100 cm. This decrease is due to the effect of the light water absorption in the fast core and a minor moderation in the fast core, consequently, the number of neutrons' contribution from the fast core to the thermal core is decreasing. At light water level of 100 cm or more the coefficient k_{21} comes to stability due to the balance of the rate diffusion of neutrons from the fast to the thermal one being equal to the rate of total absorption in the fast core. The percentage difference between the MCNP5 and Serpent results for the coupling coefficients k_{12} and k_{21} were determined as 0.54% and 0.71% respectively.

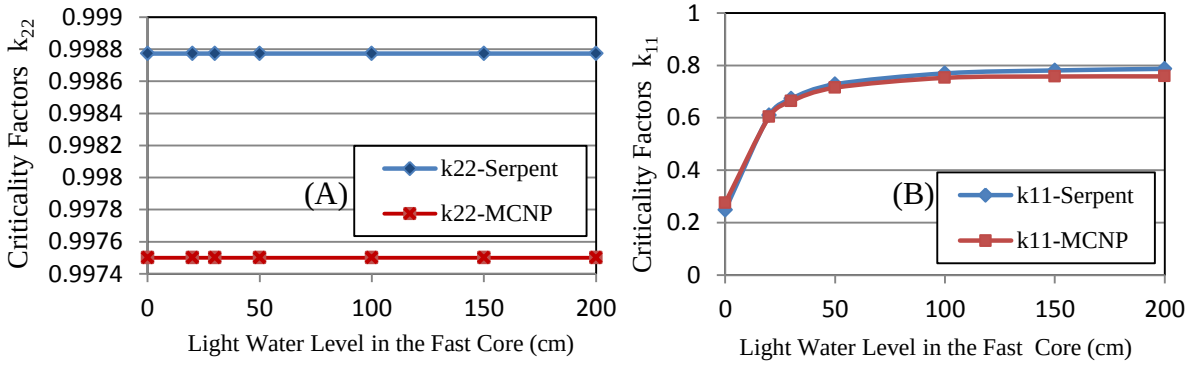

Figure 10: Criticality Factors k_{22} (Figure 10-A) and k_{11} (Figure 10-B) at Different Light Water Levels in the Fast Core with Heavy Water at 100 cm in the Thermal Core Calculated by Serpent and MCNP5.

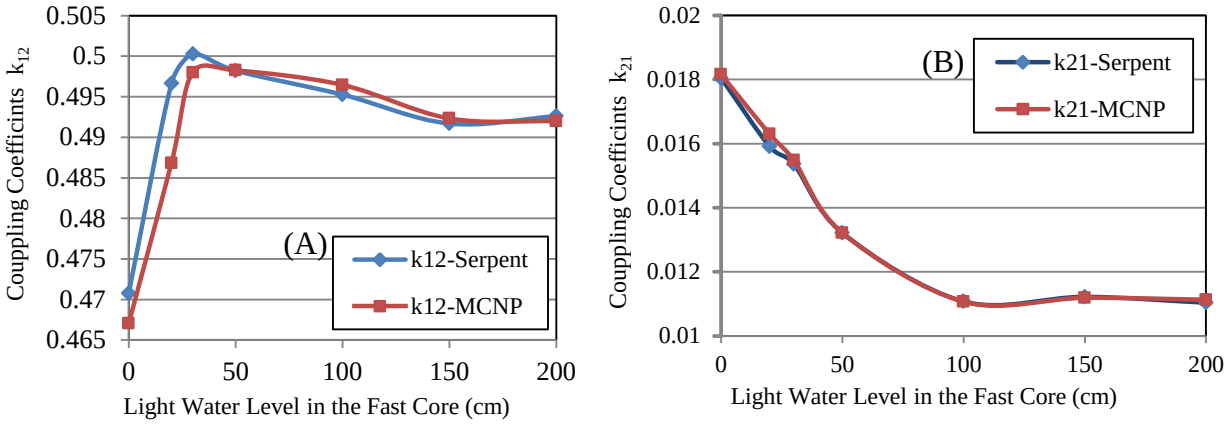

Figure 11: Coupling Coefficients k_{12} (Figure11- A) and k_{21} (Figure11- B) at Different Light Water Levels in the Fast Core with Heavy Water at 100 cm in the Thermal Core Calculated by Serpent and MCNP5.

12- In this part of the simulation, the level of light water in the fast core is fixed at 100 cm while the level of the heavy water is changed from 0 to 200 cm as shown in Figures 12 to 15. From Figure 12, one can notice the consistency of the criticality factors k_{11}, k_{22} and coupling coefficients k_{12} and k_{21} as calculated from the MCNP5 and Serpent codes. Consequently, The multiplication factors k_{eff} calculated by the coupled reactor equation, depending on these values k_{11}, k_{22}, k_{12} and k_{21}, from the two codes independently, are almost match the k_{eff} calculated with MCNP5 and Serpent independently.

13- Figure 13 presents the comparison between the multiplication factors k_{eff} values calculated directly by both Serpent and MCNP5 and those calculated with the coupled reactor equation. One can notice that the behaviour of k_{eff} curves calculated by the two codes corresponds well and are also close to the values determined with the coupled reactor theory. Table (1) describes the average percentage difference between the k_{eff} calculated by MCNP5, Serpent and the coupled reactor theory.

14- Figure 14 (A) and (B) show the close-up of the results for the criticality factors k_{22} and k_{11}. One can notice that, on the other hand, from Figure 14 (A), the criticality factor k_{22} sharply increases as the heavy water level increases because of the moderation effect, but at 100 cm, the rate of increase of k_{22} decreases gradually to a constant value. This is because of the rate of fission that equals the rate of absorption and leakage from the core. The criticality factors k_{22} from MCNP5 and Serpent are in an excellent agreement with a difference 0.23%. On the other side Figure 14 (B), as the water level increases in the thermal core, the value of k_{11} is not affected because it was calculated when the thermal core was switched off. The criticality factors k_{11} from MCNP5 and Serpent are very much in a good agreement with a difference of 2.3%.

15- Figure 15 (A) and (B) are close-up views of the change of the coupling coefficients k_{12} and k_{21} as the heavy water level increases in the thermal core when the light water level is set at 100 cm. The coupling coefficient k_{12}, from Figure 15 (A), increases sharply because of the effect of the moderation of the heavy water, i.e. more thermalization and more fission consequently more neutrons diffused from the thermal core to fast core. As the heavy water level increases

the rate of change of coupling coefficient k_{12} decreases gradually, due to the effect by the heavy water internal reflector which decreases the number of neutrons diffused from the thermal core to the fast core. In Figure 15 (B), as the heavy water increases in the thermal core, the k_{21} increases due to increasing of the number of neutrons diffused from the thermal core to the fast core due to more thermalization and fission in the thermal core. Consequently, the rate of fission in the fast core increases. The behaviour of the k_{21} curve in Figure 15 (B) is different from that of the corresponding curve in Figure 11 (B) because of the difference in the volume and amount of fuel. The percentage difference between the MCNP5 and Serpent results for the coupling coefficients k_{12} and k_{21} were 1.52% and 4.28% respectively.

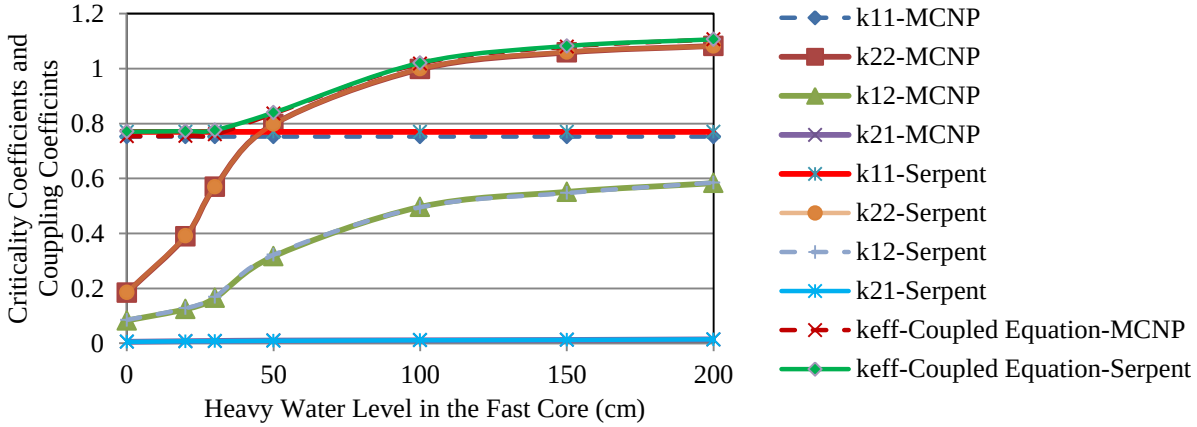

Figure 12: Criticality Factors and Coupling Coefficients at Different Heavy Water Levels in the Thermal Core with the Light Water Level at 100 cm in the Fast Core, Calculated by Serpent, MCNP5 and the Coupled Reactor Equation.

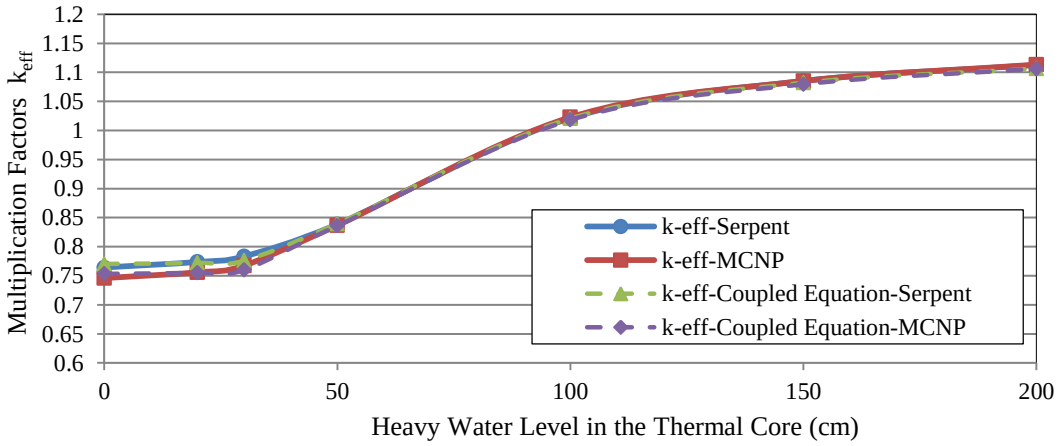

Figure 13: Multiplication Factors k_{eff} , at Different Heavy Water Levels in the Thermal Core with the Light Water Level at 100 cm in the Fast Core, Calculated by Serpent and MCNP5 and the Coupled Reactor Equation.

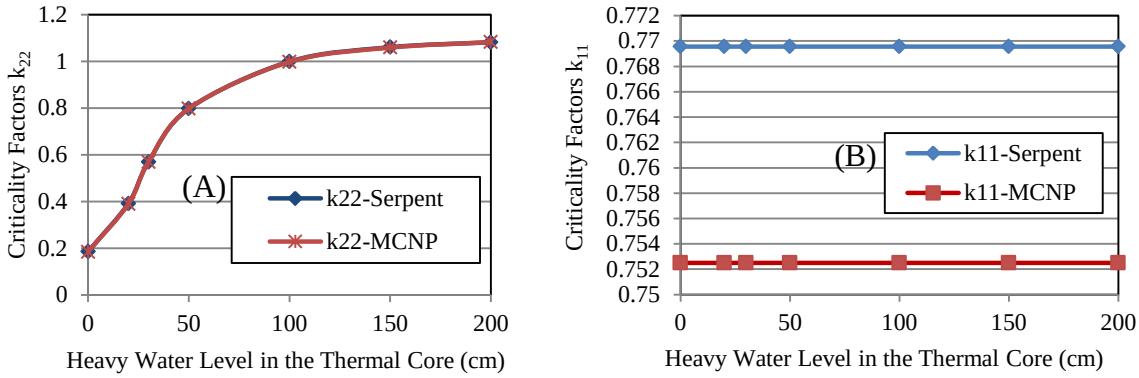

Figure 14: Criticality Factors k_{11} (Figure 14-A) and k_{22} (Figure 14-B), at Different Heavy Water Levels in the Thermal Core with the Light Water Level at 100 cm in the Fast Core, Calculated by Serpent and MCNP5.

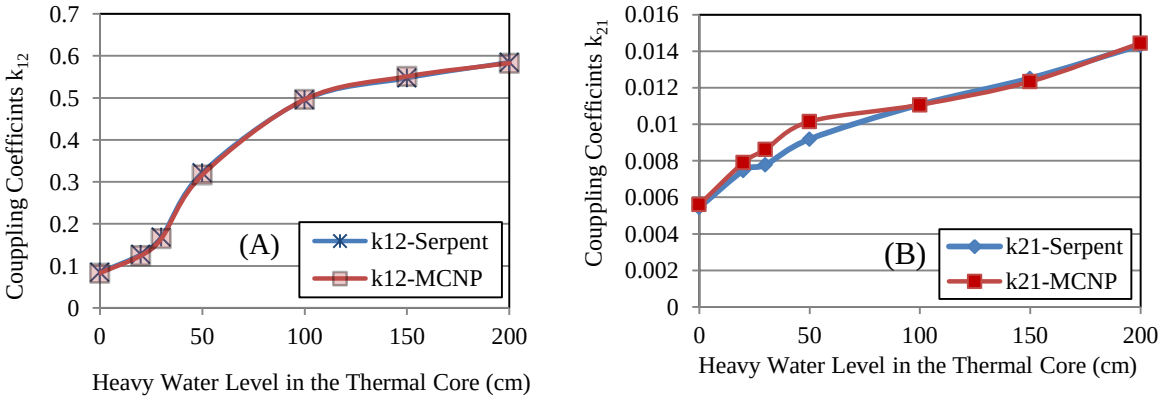

Figure 15: Coupling Coefficients k_{12} (Figure15- A) and k_{21} (Figure15- B), at Different Heavy Water Levels in the Thermal Core with the Light Water at 100 cm in the Fast Core, Calculated by Serpent and MCNP5.

6. Conclusion

The multiplication factors calculated by coupling coefficients and regional criticality factors using the coupled reactor theory agree well with those obtained directly and independently from the MCNP5 and the Serpent. There is a very good agreement between the results obtained numerically from Serpent and those from the MCNP5. Therefore, the coupling coefficients can be calculated with sufficient accuracy using these codes. The validity of the coupled reactor theory has also been verified. Therefore, the coupled reactor theory using the MCNP5, transport code, and the Serpent, continuous-energy Monte Carlo reactor physics burnup code, can be used for designing a multipoint reactor or specifically a multi-spectrum CANDU reactor.

References

[1] K.Nishihara, "Numerical Validation of the Theory of Coupled Reactors for the Heavy Water Critical Assembly DCA," vol. 36, pp. 265-272, 1999.

[2] M.S. Hussein, H.W. Bonin and B.J. Lewis, "Numerical Verification of the Theory of Coupled Reactors for a Deuterium Critical Assembly Using MCNP5," in *34th Annual Conference of the Canadian Nuclear Society*, Toronto, 2013.

[3] K. Lathrop and F. Brinkley, "Theory and use of the general geometry TWOTRAN program, LA 4432," Los Alamos National Laboratory of the University of California, NEW MEXICO, 1970.

[4] R. Avery, "Theory of Coupled Reactor," in *2nd International Conference on the Peaceful Uses Atomic Energy*, Geneva, 1958.

[5] R. Avery, "Coupled Fast-Thermal Power Breeder," *Nuclear Science and Engineering*, vol. 3, pp. 129-144, 1957.

[6] R. Avery, C.E. Branyan et.al., "Coupled Fast-thermal Power Breeder Critical Experiment," in *2nd International Conference on the Peaceful Uses Atomic Energy*, Geneva, 1958.

[7] M. Komata, "On the Derivation of Avery's Coupled Reactor Kinetic Equations," *Journal of Nuclear Science and Engineering* , vol. 38, pp. 193-204, 1969.

[8] K. Kobayashi, "Rigorous derivation of Static and Kinetic Nodal Equations for Coupled Reactors Using Transport Equations," *Journal of Nuclear Science and Technology*, vol. 28, pp. 389-398, May 1991.

[9] F. Allen et.al., "Extending the CANDU Nuclear Reactor Concept: The Multi- Spectrum Nuclear Reactor. Feasibility Study of Designing the Multi-Spectrum Nuclear Reactor Using the CANDU's Unique Features," Master degree thesis, Royal Military College of Canada, Kingston, 2009.

[10] Los Alamos National Laboratory , "Monte Carlo N–Particle Transport Code System, MCNP5 1.51.," Radiation Safety Information Computational Center, 2008.

[11] Luka Snoj, Matjaž Ravnik, "Calculation of Power Density with MCNP in TRIGA reactor," in *International Conference Nuclear Energy for New Europe 2006*, Portorož, Slovenia, 2006.